SUPPLEMENTAL MATERIAL

Kasheta et al., https://doi.org/10.1084/jem.20162084

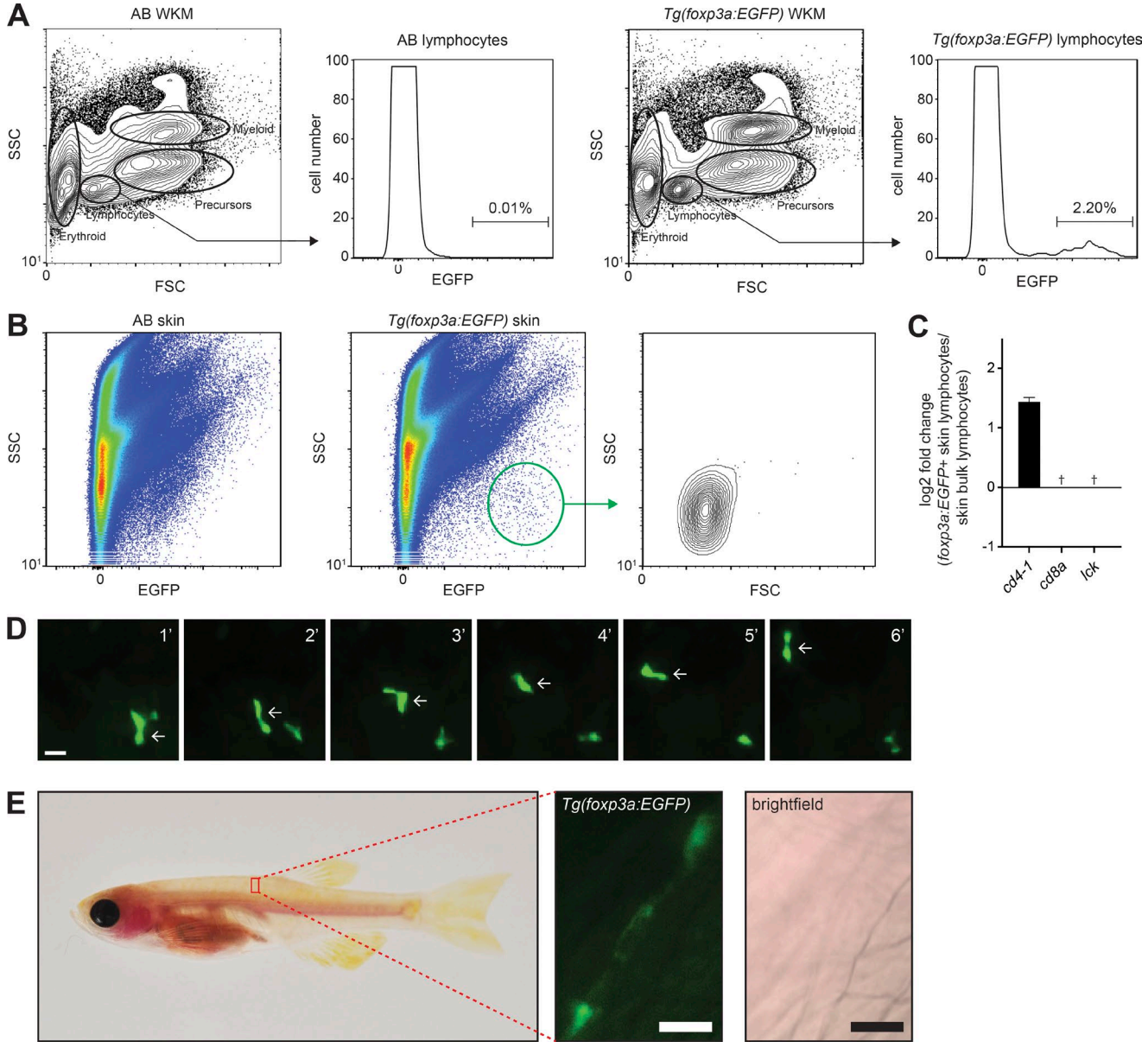

Figure S1. **Analysis of *foxp3a:EGFP*–positive cells in multiple tissues.** (A) Gating strategy for quantification of EGFP-positive lymphocytes from WKM. Related to Fig. 1 D. (B) Flow cytometry analysis of skin from representative AB and *Tg(foxp3a:EGFP)* animals. (C) qRT-PCR of selected genes in *foxp3a:EGFP* -positive thymocytes relative to bulk thymocytes. †, Expression of *cd8a* and *lck* was below the limit of detection in *foxp3a:EGFP*-positive skin lymphocytes. Error bar indicates SEM; $n = 3$. (D) Still frames from live imaging (Video 1) of a *foxp3a:EGFP*-positive cell migrating through skin (arrows). Each panel represents a 1-min interval. Bar, 10 µm. (E) *foxp3a:EGFP*-positive cells between segment of dorsal musculature. Bars, 50 µm.

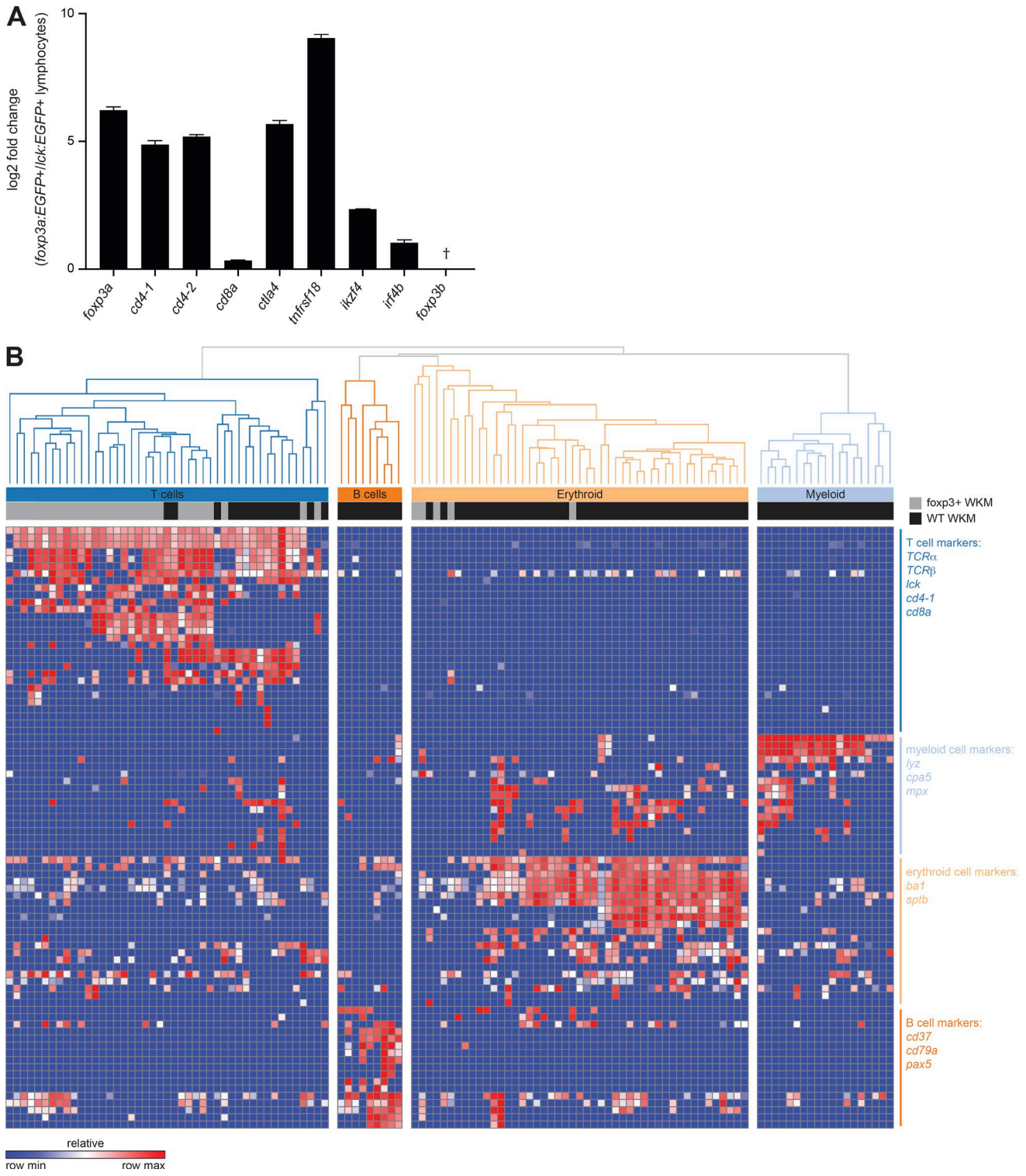

Figure S2. **qRT-PCR and single-cell analyses of *foxp3a:EGFP*-positive cells.** (A) qRT-PCR of indicated genes in *foxp3a:EGFP*-positive lymphocytes compared with lymphocytes sorted from *Tg(lck:EGFP)* animals. †, Expression of *foxp3b* was below the limit of detection in *Tg(foxp3a:EGFP)* animals. Error bar indicates SEM; $n = 3$. (B) Unsupervised hierarchical clustering using gene expression analyses of single cells. Hematopoietic lineage assignments of control WKM cells in each cluster are shown. These assignments were made based on expression of lineage-specific marker genes as well as a comparison of these expression profiles to those of cells isolated from animals with lineage-specific transgene expression (Moore et al., 2016a). Hematopoietic lineage-specific genes representing each lineage profiled are indicated (right).

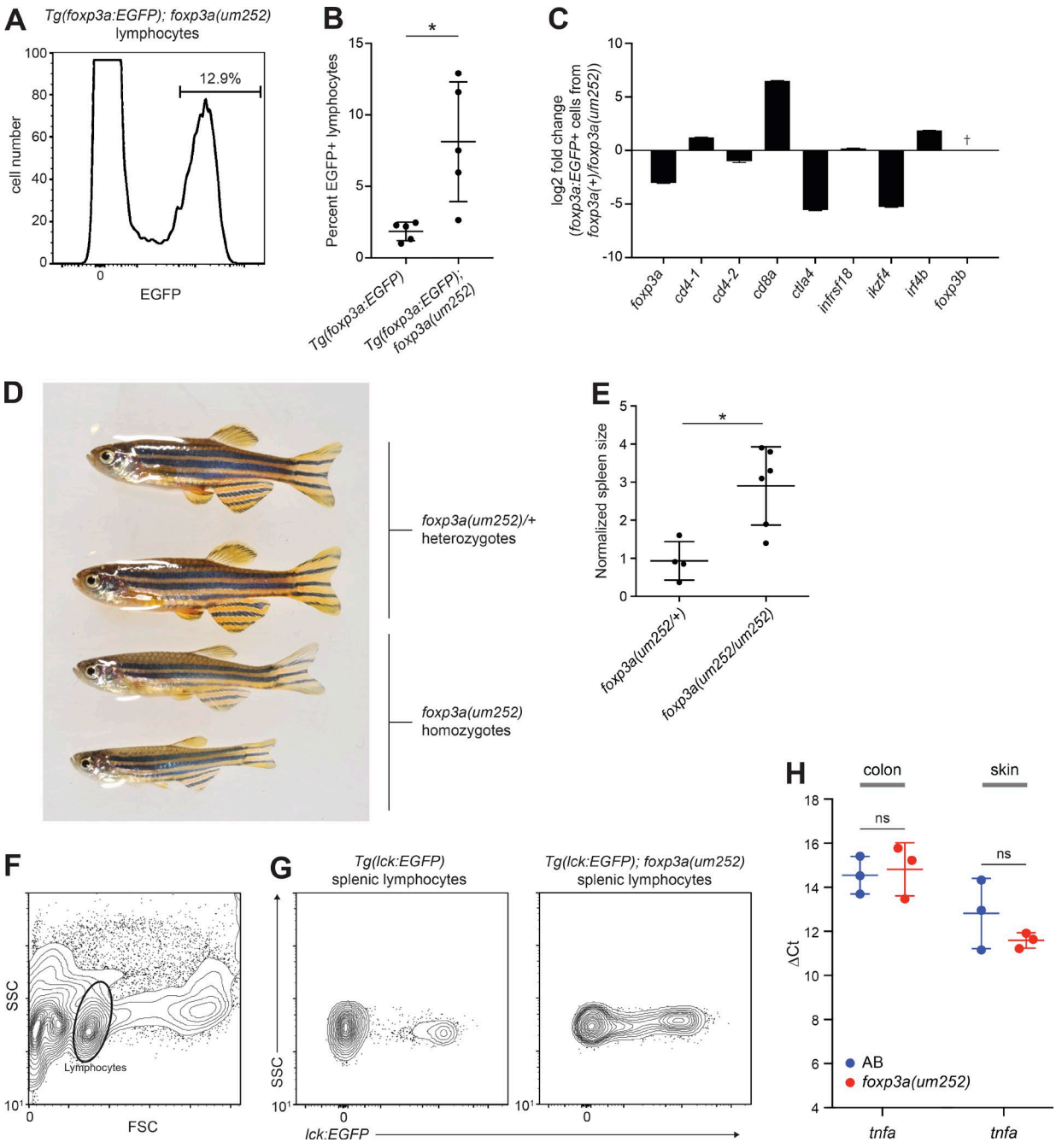

Figure S3. **Phenotypic analyses of *foxp3a* mutants.** (A) Flow cytometry analysis of WKM from a representative *Tg(foxp3a:EGFP); foxp3a(um252)* animal. Gated lymphocytes are plotted as a histogram with the percentage of *EGFP*-positive lymphocytes indicated. (B) Percentages of *foxp3a:EGFP* -positive lymphocytes, based on flow cytometry analysis, are increased in a *foxp3a(um252)* mutant ($n = 5$) compared with a wild-type ($n = 5$) background. Two-tailed Student's *t* test, *, $P < 0.05$. Error bar indicates SEM. (C) qRT-PCR of indicated genes in *EGFP*-positive lymphocytes sorted from *Tg(foxp3a:EGFP); foxp3a(um252)* and *Tg(foxp3a:EGFP)* animals. The log2 fold change of gene expression in *EGFP*-positive lymphocytes from *Tg(foxp3a:EGFP); foxp3a(um252)* animals compared with *EGFP*-positive lymphocytes from *Tg(foxp3a:EGFP)* animals is plotted. †, Expression of *foxp3b* was below the limit of detection in *EGFP*-positive lymphocytes from both *Tg(foxp3a:EGFP); foxp3a(um252)* and *Tg(foxp3a:EGFP)* animals. Error bar indicates SEM; $n = 3$. (D) Images of representative sibling *foxp3a(um252)/+* heterozygotes and *foxp3a(um252)* homozygotes. (E) Normalized spleen sizes of sibling *foxp3a(um252/+)* ($n = 4$) and *foxp3a(um252/um252)* ($n = 6$) animals. Spleen sizes ($\mu m^2 \times 10^3/mm^3$) were estimated by normalizing maximum spleen area (area at level of splenic artery) by fish volume. Two-tailed Student's *t* test, *, $P = 0.007$. (F) Flow cytometry analysis of a representative *Tg(lck:EGFP)* spleen. The lymphocyte-containing gate is indicated. (G) Gated lymphocytes from representative animals are plotted to indicate EGFP positivity. (H) qRT-PCR analysis of inflammation marker gene *tnfa*. ΔCt values were calculated relative to a *β-actin* control. Two-tailed Student's *t* test, ns, not significant. Error bar indicates SEM; $n = 3$.

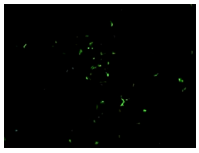

Video 1. **Long-term live-imaging of *foxp3a:EGFP*-positive cells.** Cells were imaged as described in Materials and methods. An area of skin posterior to the operculum was imaged. A time-lapse rendered video of an originally 20-min video is shown.